

## Embrittlement in Neutron Irradiated Niobium

著者	KAYANO Hideo, YAJIMA Seishi
journal or publication title	Science reports of the Research Institutes, Tohoku University. Ser. A, Physics, chemistry and metallurgy
volume	26
page range	107-116
year	1976
URL	<a href="http://hdl.handle.net/10097/27796">http://hdl.handle.net/10097/27796</a>

# Embrittlement in Neutron Irradiated Niobium\*

Hideo KAYANO and Seishi YAJIMA

*The Oarai Branch, The Research Institute for Iron, Steel and Other Metals,  
Tohoku University, Oarai-machi, Ibaraki-ken, JAPAN*

(Received September 9, 1976)

## Synopsis

This paper discusses the effect of neutron irradiation on the embrittlement of niobium. The irradiation was carried out at about 100°C to a neutron dose of  $2.9 \times 10^{20} \text{n/cm}^2$  (>1 MeV) and measurements were made of the yield stress, fracture stress and fracture strain in the temperature range from liquid nitrogen to room temperature. The interaction of dislocations produced by deformation with irradiation-induced defects was studied by transmission electron microscopy. The fracture surfaces were examined using a scanning electron microscope. The brittle fracture stress was evaluated under theory of the dislocation and by the strain-energy method. Based on the results obtained, a possible mechanism for the fracture in neutron irradiated niobium was discussed.

## I. Introduction

When metals are irradiated to neutrons, the yield strength and brittleness increase generally. For the former, there are a number of theories of Seeger<sup>(1)</sup>, Fleisher<sup>(2)</sup>, and Frank<sup>(3)</sup> et al. and others, with some experimental studies<sup>(4),(5)</sup>. For the latter, the qualitative studies from the practical standpoint are many, including a phenomenological treatment of Cottrell.<sup>(6)</sup> Microscopic studies on embrittlement of b.c.c. metals due to irradiation-induced defects are almost none, however. In the present study, therefore, niobium was irradiated using JMTR (Japan Materials Testing Reactor), and measurements of the yield stress, fracture stress and fracture strain were made in the temperature range from liquid nitrogen temperature to room temperature. The interaction of dislocations produced by deformation with irradiation-induced defects was studied by observation with a transmission electron microscopy results. The fracture was observed using a scanning electron microscope. Brittleness in irradiated niobium was discussed quantitatively on the basis of the results obtained.

---

\* The 1663th report of the Research Institute for Iron, Steel and Other Metals.

- (1) A. Seeger, 2nd Int. Conf. on Peaceful Uses of Atomic Energy Geneva, **6** (1958), 250.
- (2) R.L. Fleisher, *Acta Met.*, **10** (1962), 835.
- (3) W. Frank, *Z. Naturforsch.*, **22a** (1967), 365.
- (4) Koppenaal, T.J., Arsenault, R.J., *Phil. Mag.*, **12** (1965), 951.
- (5) D.S. Billington and J.H. Crawford, *Radiation Damage in Solids*, Princeton (1961), 100.
- (6) A.H. Cottrell, ASTM-STP-484 (1971).

## II. Experimental procedure

The specimens used are niobium polycrystal plates having chemical composition shown in Table 1. The dimensions of the specimens for the tensile test were  $0.5 \times 10 \times 50$  mm<sup>3</sup> in the rectangular part. These specimens were irradiated in JMTR to neutron fluxes of  $2.9 \times 10^{20}$  n/cm<sup>2</sup> ( $>1$  MeV) at the temperature estimated to be about 100°C.

Table 1. Chemical composition of Nb investigated. (w/o)

O	H	N	Fe	Ni	Co	Ta	C
0.007	0.0009	0.0046	<0.0010	<0.0010	<0.0010	0.090	0.0050

The irradiated specimens were then decladded in the hot laboratory of the Oarai Branch and were subjected to tensile tests at temperatures from liquid nitrogen temperature (LNT) to room temperature using an Instron type testing machine (Shimazu Autograph-500). Thin foils for transmission examination were prepared from sections of the tensile test specimens by chemical and electrical polishing. The crystallographic textures, irradiation-induced defects and dislocation structures after deformation were examined for the thin foils using a transmission electron microscope (JEOL, JEM-200A). Fracture surfaces were observed using a scanning electron microscope (JEOL, JSM-U3).

## III. Experimental results

Figure 1 shows the temperature dependences of yield stress ( $\sigma_y$ ), fracture stress ( $\sigma_f$ ) and fracture strain ( $\epsilon_f$ ) in the temperature range of LNT to room temperature for niobium polycrystals irradiated in JMTR to a fast neutron flux of  $2.9 \times 10^{20}$  n/cm<sup>2</sup> ( $>1$  MeV). The results for the unirradiated specimens are also given. The strain rate in the tensile tests was  $2 \times 10^{-5}$  sec<sup>-1</sup>. Both the yield stress ( $\sigma_y$ ) and the fracture stress ( $\sigma_f$ ) increase with irradiation, but the fracture strain ( $\epsilon_f$ ) decreases. At LNT, the irradiated specimen did not exhibit plastic elongation, but showed brittle fracture. Photo 1. shows a microstructure near the fracture surface of the irradiated specimen at LNT. The black dots indicate irradiation-induced defects, which are believed to turn into dislocation loops of the interstitial type by heat treatment at 200°C for 1 hr<sup>(7)</sup>. These defects might be the clusters of interstitial atoms. As seen in this photograph, dislocation channels take place around inclusions.<sup>(8)</sup> The channeling plane is determined to be {110}, and the Burgers vector of the dislocations in the channelings  $(a/2)$  [111]. Diameters of the inclusions are about  $0.3 \mu$  on the average. Photo. 2 shows the microstructure of the unirradiated specimen fractured under the same condition as in Photo 1. It is

(7) S.M. Ohr, R.P. Tucker and M.S. Wechsler, Trans. JIM, **9** (1968), 187.

(8) R.P. Tucker, M.S. Wechsler and S.M. Ohr, J. Appl. Phys., **40** (1969), 400.

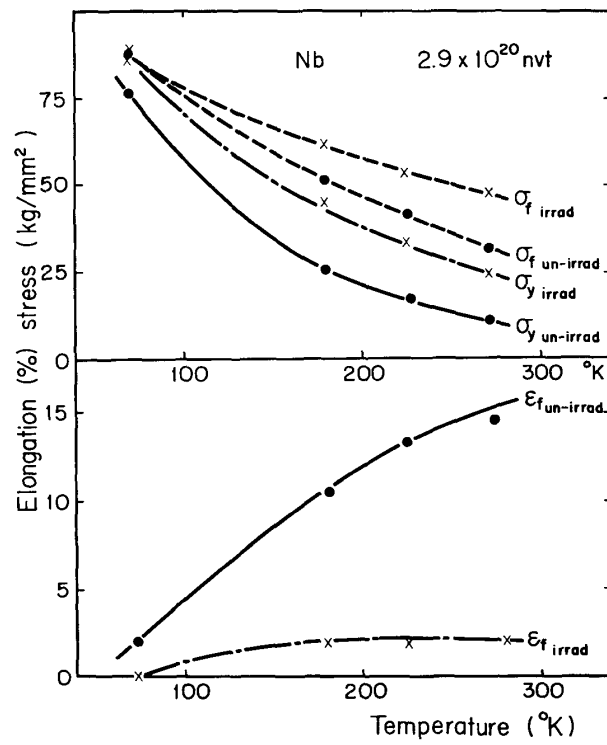


Fig. 1. Temperature dependence of true stress and true strain of irradiated, unirradiated Nb.

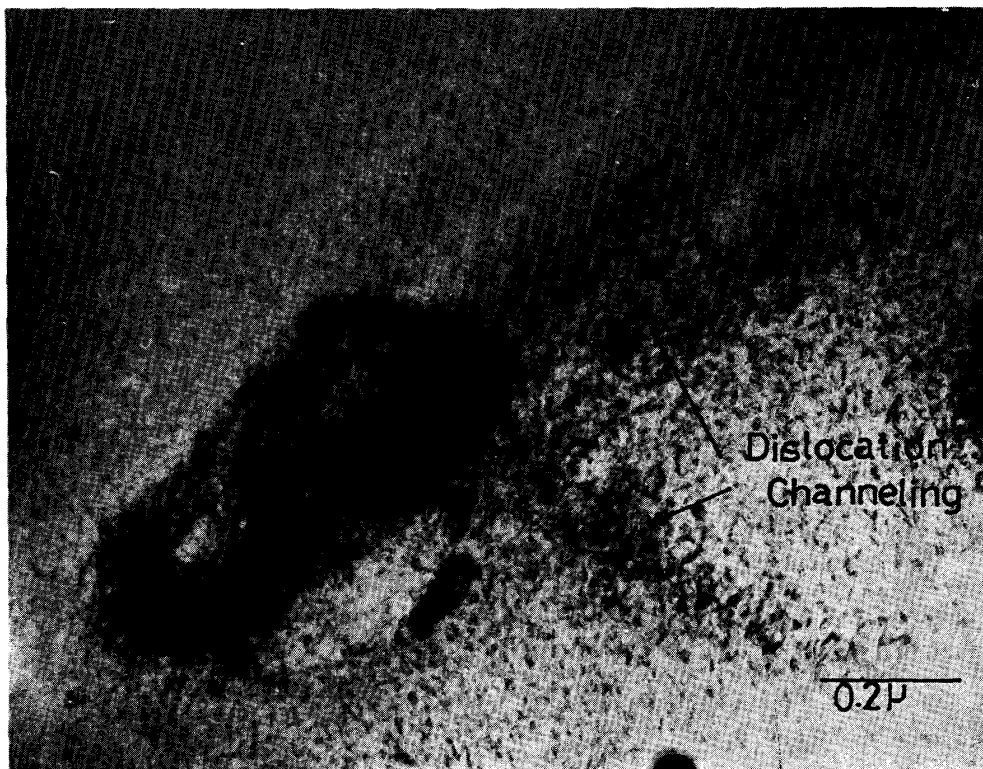


Photo. 1. Dislocation channel in neutron-irradiated Nb fractured at liquid  $N_2$  temperature.

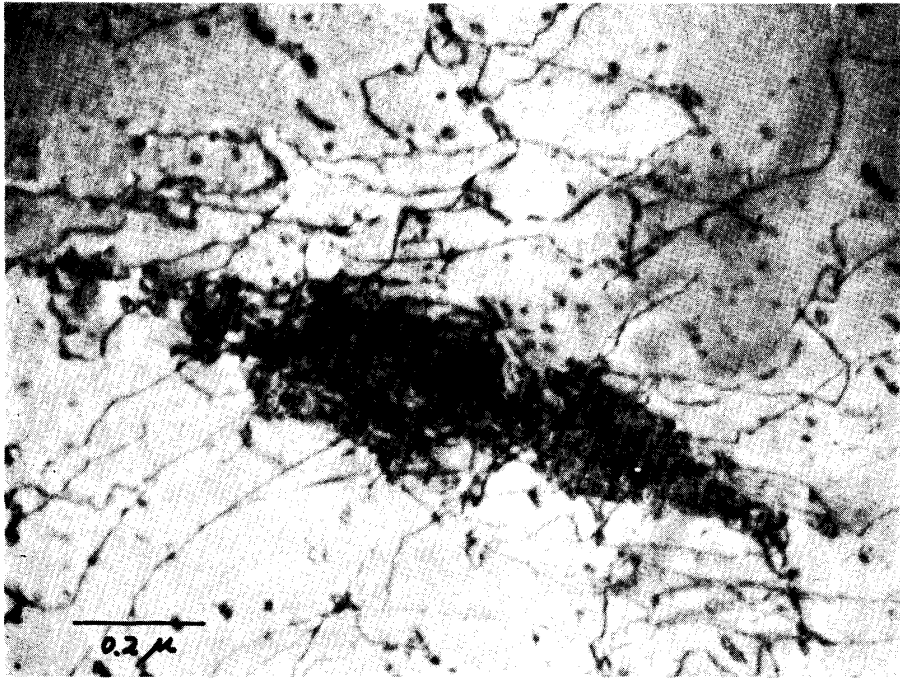


Photo. 2. Dislocation configuration in unirradiated Nb fractured at liquid  $N_2$  temperature.



Photo. 3. Dimples of unirradiated Nb fractured at liquid  $N_2$  temperature.

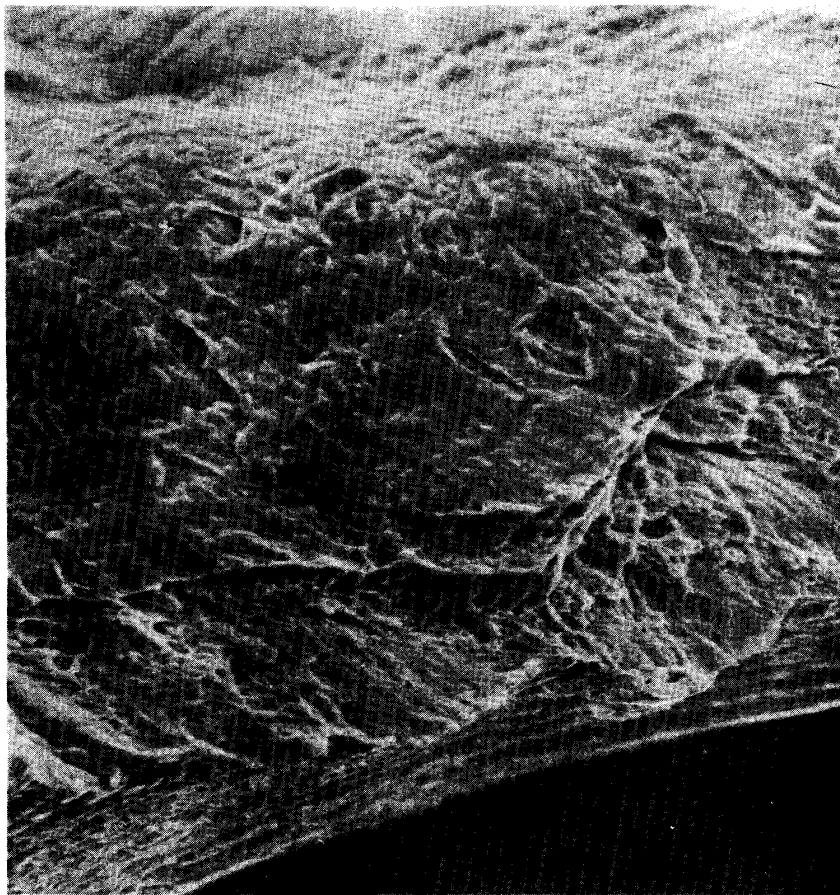


Photo. 4. Dimples and river pattern of irradiated Nb fractured at liquid N<sub>2</sub> temperature.

shown that dislocation channels are not seen and the dislocations are distributed uniformly.

Photo. 3 shows the surface of the irradiated specimen fractured at LNT, which is observed with the scanning electron microscope. The surface marking show generally the river pattern; characteristic of a cleavage fracture, and the dimples appear only on the edge of the fracture surface. In the unirradiated specimen, on the other hand, the entire fracture surface is covered with dimples, as seen in Photo. 4. The fracture surface is rather planar in the irradiated specimen, but there is no appreciable difference in the density and size of dimples between the irradiated and the unirradiated specimens. In the irradiated specimen the density of dimples was estimated from the number of dimples formed near the periphery of the fracture surface because the dimples occur only on the edge.

#### IV. Discussion

##### 1. Formation of microcracks and dimples

The mechanism of microcrack formation is considered have on the basis of the experimental results on irradiated niobium specimens.

In Cottrell's model of brittle fracture, the dislocations of  $a/2$   $[111]$  type Burgers vector coalesce to form a dislocation of the  $[100]$  type Burgers vector due to cross-slip, etc., resulting in brittle fracture. Stroh<sup>(9)</sup> has shown that a pure  $[100]$  dislocation may not be an effective barrier. Although other models have been proposed in refs. (10) and (11) etc., no definite theory of the brittle fracture based upon the dislocation theory of stress concentration has been established yet. The quantitative analysis of the irradiation brittle fracture based on the irradiation-induced defects is not available in the literature. A model, therefore for a b.c.c. metal, which is based on the experiment with irradiated niobium, will be considered here.

There is no difference in the density and size of dimples between the irradiated and unirradiated specimens as already described. The microcrack seems to be produced as follows. A non-metallic inclusion acts as the source of stress concentration in both the irradiated and unirradiated specimens. While the dislocations multiply at this site, a vacancy loop develops and thereby the nucleation of a microcrack or a dimple occurs. As indicated in Fig. 2, the dislocation occurs at a site where the stress concentration is considerable, due to the external stress. The Burgers vector of this dislocation is a  $a/2$   $[111]$  type perfect dislocation.

The edge component moves forward by external force, while the screw component rotates rather than the forward movement since the stress concentra-

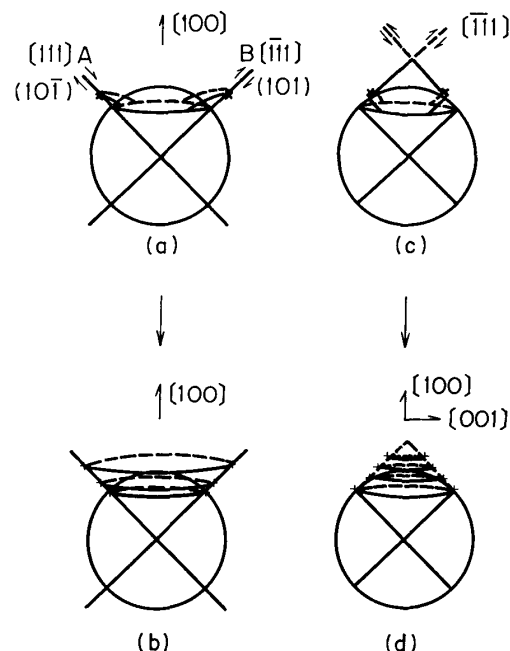


Fig. 2. Model of microcrack or dimple nucleation.

(9) A.N. Stroh, *Fracture* (1959) 117 (Proc. Intern. Conf. (Swampscott)).

(10) G.T. Hahn and A.R. Rosenfield, *Acta Met.*, **14** (1966), 1815.

(11) F. Terasaki, *Metaux et Corrosion*, **1** (1967), 68.

tion around the inclusion is large, as indicated by A and B in Fig. 2 (a).<sup>(12),(13)</sup> The semi-dislocation loop nucleated in A side is linked with the semi-dislocation loop in B side by the stress concentration around the inclusion and thus loops becomes a vacancy type loop as shown in Fig. 2 (b). The dislocation in the direction B of Fig. 2 (a) rotates similarly. Merger of the vacancy-type loops results in the occurrence of a microcrack or a dimple by the stress concentration of the applied external stress. A similar mechanism may be considered as shown in Fig. 2 (c) and (d). The mechanism may also be operative in a b.c.c. metal, like niobium having the  $a/2$   $[111]$  type Burgers vector, as shown in Fig. 2 (c) and (d). This model equally applies well to the case of a f.c.c. metal. In this case, the vacancy loops of the  $a/2$   $[10\bar{1}]$  and  $a/2$   $[011]$  types are formed, and in merging, they develop into Lomer-Cottrell's sessile dislocation of the  $a/2$   $[110]$  type.

In the ductile fracture with dimples and the brittle fracture without dimples, a dislocation develops at the site where stress concentration is considerable, such as that around an inclusion. These dislocations coalesce to form a dislocation loop of the vacancy type as described before. In the case of a ductile fracture, it grows into a dimple, and into a microcrack in the case of a brittle fracture. That is, in the initial stage of vacancy-type dislocation loop formation, if the stress concentration concerned has attained a cleavage value, there occurs a cleavage-type fracture.

The cleavage-type brittle fracture occurs generally as follows. The resistance in a dislocation contributing to the internal deformation of a crystal is large, or the dislocations are small in number due to the inability of multiplication. The structure cannot then undergo an external stress or deformation. The result is an increase of the stress concentration in dislocation loops of the  $[100]$  type formed around the inclusion. The stress value for the cleavage-type fracture is thus attained, leading to the fracture.

The ductile fracture, on the other hand, takes place as follows. The resistance in a dislocation is insignificant and the multiplication of dislocations is also large. Plastic deformation thus readily occurs for an external stress. The dislocation loops of the  $[100]$  type around an inclusion continues to multiply, without attaining a cleavage stress. It grows into a dimple. These dimples then coalesce and lead to the fracture. In a quantitative treatment of the ductile fracture with dimples, it is necessary to consider the stress concentration of a dislocation in dimple and the stress relaxation due to multiplication of dislocations in the matrix and their movement. In the case of a brittle fracture, however, the stress relaxation due to the dislocation movement in the matrix and its multiplication is small compared with the stress concentration around an inclusion; therefore, the relieving may be neglected. The following is a quantitative treatment dealing mainly with a cleavage-type fracture in irradiated niobium without growth of dimples.

---

(12) H. Kayano, J. of Japan Inst. Met., **31** (1967), 310.

(13) M.F. Ashby and L. Johnson, Phil. Mag., **20** (1969), 1009.



## 2. Irradiation brittleness

The brittle fracture stress of an irradiated specimen will be considered.<sup>(14)</sup> In Fig. 3, the concentration stress  $\tau_c$  at a point  $\delta_c$  away from the inclusion of radius  $R$  and elastic modulus  $E$  is calculated as<sup>(14)</sup>

$$\tau_c = (\tau_a - \tau_f) \frac{1}{2} \frac{\Delta E}{E} \sqrt{\frac{2R}{\delta_c}} + \tau_f, \quad (1)$$

where  $\tau_f$  is the frictional stress of the dislocation,  $\Delta E$  the difference in elastic modulus between the matrix and the inclusion,  $\tau_a$  the applied external stress. Assuming the diameter  $d_i$  and density  $n_i$  for radiation defects in the irradiated specimen, the frictional stress  $\tau_f$  is given by<sup>(15)</sup>

$$\tau_f = \tau_y + \frac{1}{2} \alpha' \mu b (\Sigma n_i d_i)^{1/2}, \quad (2)$$

with

$$\tau_y = \tau_p \left(1 - \frac{T}{T_0}\right)^2,$$

Here,  $\alpha'$  is the parameter ranging from 0 to 1,  $\mu$  the shear modulus,  $b$  the Burgers vector,  $\tau_y$  the temperature-dependent yield stress of the crystal,  $\tau_p$  the effective stress at 0°K,  $T_0$  the temperature where the thermal component of stress becomes zero,  $N$  the average dislocation density in deformation, and  $\alpha$  a constant.

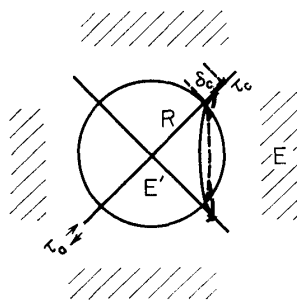


Fig. 3. Stress concentration around an inclusion in a crystal.

If a microcrack is formed by the  $n$  dislocation loops of Burgers vector  $b$  due to the stress  $\sigma$  around an inclusion of radius  $R$ ,  $\sigma$  is given by<sup>(16)</sup>

$$\sigma = \frac{\mu n b}{\alpha(1-\nu)R}, \quad (3)$$

where  $\alpha$  and  $l$  are constants equal to  $1-\nu$  for the edge and screw dislocations, respectively.

(14) A.H. Cottrell, *The Relation between the Structure and Mechanical Properties of Metals* **2**, Her Majesty's Stationery off (1963), 456.

(15) H. Kayano and S. Yajima, *Nuc. Sci. Tec.*, **13** (1976), to be published.

(16) A.H. Cottrell, *Trans. AIME*, **212** (1958), 192.

The energy, when the microcrack of length  $L$  increases by  $r$  due to the external applied normal stress  $\sigma_{ap}$ , is given<sup>(17)</sup> by

$$W = \frac{\mu n^2 b^2}{4(1-\nu)} \ln\left(\frac{4L_0}{r}\right) + 2\gamma r - \frac{\sigma_{ap} n b}{2} (L+r) + \frac{\pi(1-\nu)\sigma_{ap}^2 L^2}{8\mu} - \frac{\pi(1-\nu)\sigma_{ap}^2 (L+r)^2}{8\mu} \quad (4)$$

$L_0$  is the effective radius of the stress field for the dislocation,  $\gamma$  the effective surface energy of the matrix, and  $\nu$  Poisson's ratio of the matrix. If a microscopic crack is to be formed, with  $dw/dr = 0$ , and by the condition  $D \leq 0$ , where  $D$  is the discriminant of the quadratic equation in  $r$ ,

$$\sigma_{ap}^2 R + \frac{4}{\pi} \alpha \sigma_{ap} \sigma R - \frac{8\gamma\mu}{\pi\sqrt{2}(1-\nu)} = 0 \quad (5)$$

From eqs. (1) and (5), the fracture stress,  $\sigma_{frac}$ , becomes

$$\sigma_{frac} = \left\{ \left( \frac{2\sigma}{\pi} \right)^2 + \frac{8\mu\gamma}{\sqrt{2}\pi(1-\nu)R} \right\}^{1/2} - \frac{2\sigma}{\pi}, \quad (6)$$

with

$$\sigma = 2\tau_f + \frac{E}{\Delta E} \sqrt{8\delta_c} (\tau_c - \tau_f) R^{-1/2}. \quad (7)$$

The experimental results for Nb will be compared with the calculated ones. Fig. 4 shows the distribution of irradiation-induced defects in the irradiation to  $2.9 \times 10^{20}$  n/cm<sup>2</sup>. The distribution of radiation defects is given by

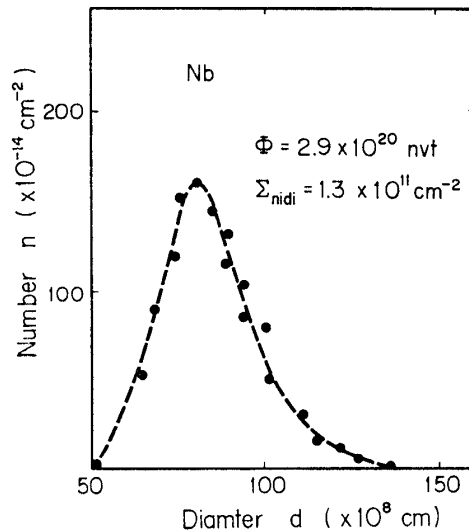


Fig. 4. Density of defects as a function of diameter in irradiated Nb.

(17) E.A. Almond, D.H. Timbres and J.D. Embury, *Fracture*, Chapman and Hall (1969), 253.

$$\Sigma n_i d_i = 1.3 \times 10^{11} \text{ cm}^{-2}. \quad (8)$$

For  $R = 0.3\mu$ ,  $\tau_c = \mu/47$ ,  $a_1 = E/\Delta E \sim 1$ ,  $\gamma = \mu b/8^{(18)}$ ,  $\sigma_c \sim 2 \times 10^{-7}$  cm and  $\alpha \sim 1$ , agreement is fairly good between experiment and calculation in the irradiated specimen as seen in Table 2. The results are given for the polycrystal. In the results obtained by Ohr et al. for the single crystal<sup>(7)</sup>, agreement is also good between calculation and experiment.

Table 2. Comparison of the experimental data with theoretically expected values for irradiated and unirradiated Nb.

Fluence (nvt)	$2.9 \times 10^{20}$ (present)	$2.8 \times 10^{17}$ (Ohr et al.)
$\sigma_{frac. irradi}$ (kg/mm <sup>2</sup> ) Cal.	72	65
Exp. (kg/mm <sup>2</sup> )	80	58

## V. Conclusions

Niobium was irradiated by JMTR to a fast neutron flux of  $2.9 \times 10^{20}$  n/cm<sup>2</sup> (>1 MeV), and the yield stress, fracture stress and fracture strain were measured in the temperature range from liquid nitrogen temperature to room temperature. From the results obtained, the embrittlement in neutron-irradiated b.c.c. metals was discussed.

A nonmetallic inclusion or surface ledge is considered to act as the source of stress concentration. While a dislocation develops at this site, a vacancy loop is formed, and eventually the nucleation of a microcrack or a dimple takes place. The mechanism of fracture of a neutron-irradiated b.c.c. metal were studied in the theory of the dislocation in terms of the strain energy method.

Calculations explain well the fracture stress in the niobium irradiated with JMTR.

(18) D. McLean, *Mechanical properties of metals*, John Wiley (1962), 254.